Journal of Computer-Aided Molecular Design, 5 (1991) 95–106
ESCOM



J-CAMD 106

# Molecular level model for the agonist/antagonist selectivity of the 1,4-dihydropyridine calcium channel receptor

David A. Langs[a,*], Yong Wha Kwon[b], Phyllis D. Strong[a] and David J. Triggle[b]

[a]*Department of Molecular Biophysics, Medical Foundation of Buffalo, Inc., Buffalo, NY 14203, U.S.A.*
[b]*Department of Biochemical Pharmacology, School of Pharmacy, State University of New York, Amherst Campus, Buffalo, NY 14260, U.S.A.*

Received 6 April 1990
Accepted 25 June 1990

*Key words:* Calcium channel receptor; Nifedipine activators; Channel gating mechanism; Crystal structures

## SUMMARY

Crystal structures of the 1,4-dihydropyridine (1,4-DHP) calcium channel activators Bay K 8643 [methyl 1,4-dihydro-2,6-dimethyl-3-nitro-4-(3-nitrophenyl)-pyridine-5-carboxylate], Bay O 8495 [methyl 1,4-dihydro-2,6-dimethyl-3-nitro-4-(3-trifluoromethylphenyl)-pyridine-5-carboxylate], and Bay O 9507 [methyl 1,4-dihydro-2,6-dimethyl-3-nitro-4-(4-nitrophenyl)-pyridine-5-carboxylate] were determined. The conformations of the 1,4-DHP rings of these activator analogues of Bay K 8644 [methyl 1,4-dihydro-2,6-dimethyl-3-nitro-4-(2-trifluoromethylphenyl)-pyridine-5-carboxylate] do not suggest that their activator properties are as strongly correlated with the degree of 1,4-DHP ring flattening as was indicated for members of the corresponding antagonist series. The solid state hydrogen bonding of the N(1)-H groups of the activators is not, unlike that of their antagonist counterparts, to acceptors that are directly in line with the donor. Rather, acceptor groups are positioned within ± 60 degrees of the N(1)-H bond in the vertical plane of the 1,4-DHP ring. Previously determined structure–activity relationships have indicated the importance of this N(1)-H group to the activity of the 1,4-DHP antagonists. Based on these observations, a model is advanced to describe the 1,4-DHP binding site of the voltage-gated $Ca^{2+}$ channel and its ability to accommodate both antagonist and activator ligands.

## INTRODUCTION

Interest in the 1,4-dihydropyridine (1,4-DHP) class of $Ca^{2+}$ channel ligands has been markedly increased by the discovery of activator analogues of the antagonist nifedipine [1]. These activators (Fig. 1), which include the prototype Bay K 8644 [methyl 1,4-dihydro-2,6-dimethyl-3-nitro-4-(2-trifluoromethylphenyl)-pyridine-5-carboxylate], closely resemble the antagonists of the nifedipine series and yet are potent activators of the L-class of voltage-dependent $Ca^{2+}$ channels [2–4].

*To whom correspondence should be addressed.

0920-654X/$ 5.00 

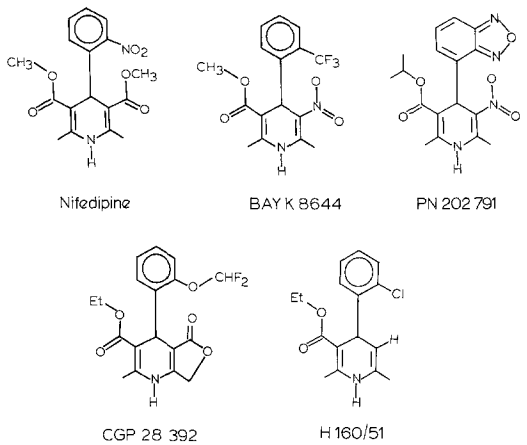


Fig. 1. Structural formulae of selected antagonist and activator analogues of nifedipine.

Considerable effort has been devoted to the determination of structure–activity relationships of the 1,4-DHP antagonists, and the importance of electronic, lipophilic and steric interactions has been delineated [4–10]. In contrast, little information is available for the structure–activity relationships of the 1,4-DHP activators. However, the competitive radioligand binding interactions of the activator and antagonist series are consistent with their interaction with at least one common site [11]. Bay K 8644 has been used extensively to explore the basis of $Ca^{2+}$ channel activation and to define biochemical sites of action. The behavior of some chiral 1,4-DHP analogues, where the enantiomers may exhibit either activator or antagonist properties, draws attention to the importance of absolute configuration at the ligand–receptor interface. *S*- and *R*-Bay K 8644 show activator and antagonist properties respectively, with the more potent activators predominating in the racemate [12,13]. Similar observations have been made for other pairs of drugs including PN 202 791 and H 160/51 (Fig. 1) [13–15].

Previous studies of the crystal structures of 1,4-DHP antagonists bearing *ortho*- or *meta*-substituents in the phenyl ring have indicated that the activities correlate with the planarity of the 1,4-DHP ring, activity increasing with increasing ring planarity [4,9,16]. The crystal structures of Bay K 8644, CGP 28 392 [17] and PN 202 791 [18] do not, however, support this argument. Models of drug interactions at the 1,4-DHP receptor have considered differences in ligand–receptor hydrogen bonding patterns to be differentiating features for activator and antagonist action. The present study extends these observations to include three additional analogues of Bay K 8644 whose biologic activities have been reported previously [19]. These three analogues, Bay K 8643, Bay O 8495 and Bay O 9507 (Fig. 2) exhibit similar potencies as activators in smooth and cardiac muscle tension studies and in radioligand binding studies in membrane preparations from the same tissues. However, the limited data available suggest that the influence of the aromatic substitution pattern may be less marked in the activator than in the antagonist series. Thus, comparison of the activities of Bay O 8495, Bay K 8643 and Bay O 9507, which are the respective 3-$NO_2$, 3-$CF_3$ and 4-$NO_2$ phenyl-substituted analogues of this activator series, shows a modest 5–16-fold spread in activities. In the antagonist series the 4-$NO_2$ substitution causes a greater than 1000-fold loss of activity [3–5,7].

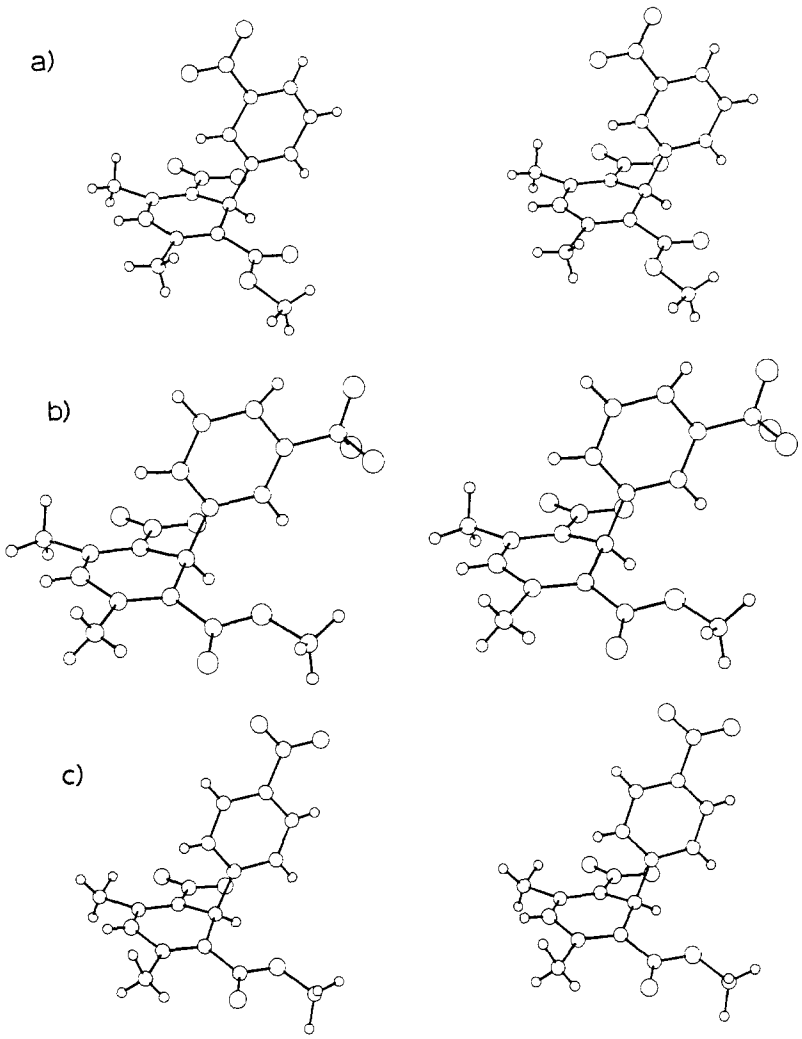


Fig. 2. Stereoviews of the solid state structures of the three Bayer activator analogues: (a) Bay K 8643 (I); (b) Bay O 8495 (II); and (c) Bay O 9507 (III).

## METHODS

*Single crystal X-ray diffraction analyses*

Crystal structures of the following activator analogues (Bayer A.G., Wuppertal) were analyzed: Structure I, Bay K 8643 [methyl 1,4-dihydro-2,6-dimethyl-3-nitro-4-(3-nitrophenyl)-pyridine-5-carboxylate]; Structure II, Bay O 8495 [methyl 1,4-dihydro-2,6-dimethyl-3-nitro-4-(3-trifluoromethylphenyl)-pyridine-5-carboxylate]; and Structure III, Bay O 9507 [methyl 1,4-dihydro-2,6-dimethyl-3-nitro-4-(4-nitrophenyl)-pyridine-5-carboxylate]. Suitable crystals were obtained by evaporation from ethylacetate (crystal I, 0.10 × 0.12 × 0.62 mm), acetone (crystal II, 0.10 × 0.20 × 0.60 mm), and acetone/$H_2O$ (crystal III, 0.20 × 0.35 × 0.40 mm). X-ray diffraction data for

crystals I and II were recorded on an Enraf-Nonius CAD-4 automated diffractometer using Ni-filtered CuKα radiation (1.5418Å); data for structure III were measured on a Nicolet P3 automated instrument using Nb-filtered MoKα radiation (0.7107 Å). Lattice constants and orientation matrices were optimized by a least-squares fit of 25 well-centered reflections for each structure. The structures were phased by direct methods and refined by full matrix least-squares iterations [20]. Nonhydrogen atoms were anisotropically refined. All data for which $F \geqslant 2\sigma(F)$ were considered observed and used in the refinement. The variance of each $F$ was determined by the method of Stout and Jensen [21], with an instability correction of $P = 0.02$ for structure I and $P = 0.03$ for structures II and III. Unit cell data and least-squares refinement results are summarized in Table 1.

*Computer graphics and receptor modeling studies*

Both Corey–Pauling–Koltun (CPK) molecular models (The Ealing Corporation, Cambridge, MA) and the computer graphics program package of SYBYL software routines (Tripos Asso-

TABLE I
UNIT CELL DATA AND REFINEMENT RESULTS FOR THE THREE STRUCTURES*

| Compound | 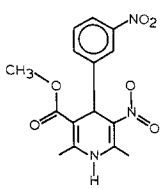 (I) | 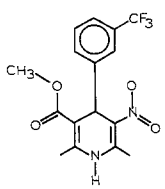 (II) | 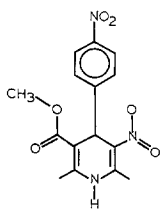 (III) |
|---|---|---|---|
| Space Group | $P2_1/c$ | $P2_1/c$ | C2/c |
| a | 11.524(1) | 11.789(2) | 20.141(3) Å |
| b | 11.462(1) | 11.516(2) | 10.308(2) Å |
| c | 12.588(1) | 12.674(2) | 15.876(2) Å |
| β | 112.93 (1) | 107.95 (1) | 99.57 (2) ° |
| V | 1531.4 (5) | 1636.9 (9) | 3250 (2) Å$^3$ |
| Z | 4 | 4 | 8 |
| Radiation | CuKα | CuKα | MoKα |
| Maximum 2Θ | 150.0 | 154.0 | 50.0 ° |
| Nref ($>2\sigma F^2$) | 3183(2916) | 3390(2685) | 2879(1858) |
| $R$ | 0.050 | 0.095 | 0.085 |
| $R_w$ | 0.062 | 0.100 | 0.077 |
| $S$ | 2.48 | 2.69 | 2.42 |
| $<\sigma$(C-C)$>$ | 0.003 | 0.005 | 0.007 Å |
| $<\sigma$(C-C-C)$>$ | 0.1 | 0.3 | 0.4 ° |
| $<\sigma$(C-H)$>$ | 0.02 | 0.06 | 0.05 Å |
| $\sigma<$(C-H)$>$ | 0.06 | 0.06 | 0.09 Å |

$R = \Sigma||Fo|-|Fc||/\Sigma|Fo|$, $R_w = [\Sigma w(|Fo|-|Fc|)^2/\Sigma w|Fo|^2]^{1/2}$,
$S = [\Sigma w(|Fo|-|Fc|)^2/(n-m)]^{1/2}$

*Atomic coordinates have been deposited with the Cambridge Structural Database, Cambridge Crystallographic Centre, Cambridge, CB2 1EW, U.K.

ciates, Inc., St. Louis, MO) were used to explore various receptor-state binding models based on our previously hypothesized model correlating the potency and tissue selectivity of nifedipine-analogue $Ca^{2+}$ channel inhibitors [22]. α-Helical segments from DHP-sensitive $Ca^{2+}$ channel $\alpha_1$-subunit sequence reported for rabbit skeletal muscle [23] were generated and modeled using the SYBYL BIOPOLYMER subroutine; crystallographic coordinates of the Bayer activators and other antagonist analogues were introduced via the CRYSIN subroutine. Molecular docking and receptor site adjustments were performed using the SYBYL subroutines TWIST to alter torsion angles and MONITOR to actively display potential intermolecular hydrogen bond and van der Waals contact distances. Full geometry energy minimizations were performed using the MAXIMIN2 program module, employing the TRIPOS basis set of force field parameters. The average (RMS) adjustments of the atomic positions seldom exceeded $\pm 0.05$ Å from the initial manually adjusted model as a result of these energy minimizations.

## RESULTS

Stereoviews of the molecular structures of the three Bayer activators are shown in Fig. 2. The absolute conformations of these molecules may be described in nautical terms relative to the boat conformation of the DHP ring and the axial or 'flagpole' orientation of the aryl ring, and whether asymmetrical DHP ring substituents are connected to the 'port' (left-hand) or 'starboard' (right-hand) side of the boat. The DHP nitro groups of the Bayer analogues in Fig. 2 are depicted on the 'port' or left-hand-side of the boat, which is consistent with the absolute *S*-configuration determined for $Ca^{2+}$ channel activation [12,14].

The three Bayer activator structures exhibit molecular conformational features that are similar to those reported for Bay K 8644. These include (i) a flattened 1,4-DHP boat conformation; (ii) a flagpole-oriented aryl ring that is coplanar with the N(1)-C(4) vertical symmetry plane of the DHP boat; and (iii) a relative lengthening of the C(2)=C(3) double bond coupled with a shortening of the adjacent N(1)-C(2) and C(3)-N(3) single bonds, which indicates a delocalization of electrons from N(1) of the DHP ring to N(3) of the 3-nitro group for all three compounds. This partial double bond character of the DHP-$NO_2$ bond would enhance the coplanarity of the $NO_2$ group with the adjoining bonds of the DHP ring, relative to a DHP ester linkage, and is consistent with the pattern proposed by Mahmoudian and Richards [24] for differentiating between ligand activators and inhibitors of $Ca^{2+}$ channel permeability.

The 3-nitrophenyl analogue (I) has an unexpected *ap* phenyl ring orientation which places the *meta*-nitro substituent directly above the 1,4-DHP ring, rather than in the forward bowsprit orientation that has been noted for all but three of the more than 35 nifedipine analogues, activators and antagonists, for which crystal structures have been determined [8,18,25]. Although the *sp* phenyl ring conformation clearly predominates, it should be noted that our published receptor model has the ability to bind equally well to *ortho*- and *meta*-substituted analogues which have either phenyl ring orientation [22].

The degree of 1,4-DHP ring planarity noted for these three activators, as indicated by the sum of the magnitudes of its six DHP ring torsion angles, are 60, 77 and 87 degrees, respectively. This compares to values of 39, 47 and 78 degrees for Bay K 8644, CGP 28 392 and PN 202 791, respectively. Semilogarithmic plots of these torsional sums versus reported pharmacologic activities and radioligand binding affinities [19] do not appear to be as linear as those observed for the related

antagonist series [8,9,16]. This result is consistent with the unusual chiral sensitivity and state-dependent interactions exhibited by calcium channel activators as compared to their antagonist analogues.

Structures I–III and Bay K 8644 are stabilized by a hydrogen bond (2.94 ± 0.04 Å) donated to O(33), the nitro group oxygen which is *cis* to the C(2)=C(3) double bond. In structure III this is provided by the water of crystallization, and in the remaining structures by the amine group of symmetry-related molecules. Electrostatic contacts to the oxygen atoms of the ester group are appreciably longer (3.30 ± 0.08 Å), clearly indicating a preference for hydrogen bond formation with the nitro group.

## DISCUSSION

### *Role of the 1,4-DHP amine group*

Studies of the structure–activity relationships of the 1,4-DHP analogues have revealed the importance of the N(1)-H group to activity. In its absence antagonist activity is eliminated or reduced dramatically [3–5]. This suggests, since this group is not ionized at physiological pH, that hydrogen bonding interactions to an acceptor group are of critical importance. A review of the more than 30 known crystal structures of analogues of nifedipine reveals there is no instance in which the N(1)-H function does not form a hydrogen bond in the solid state [4]. At least 90% of the structures have only one hydrogen bond contact less than 3.5 Å to the N(1)-H group, and this dominant interaction is invariably located along the line of sight of the N(1)-H bond. A comparison of 19 potent antagonists and 8 relatively weak antagonists showed that, because of the varying degree of 1,4-DHP ring pucker, the locus of these hydrogen bonding contacts lies in the extended N(1)-C(4) vertical plane of the 1,4-DHP ring. The preferred positions of the acceptors for the potent antagonist were found to be lower in this plane than those for the weakly active compounds [4,22]. These observations formed the basis of a hypothesis in which it was proposed that the channel state to which antagonists preferentially bound contained a hydrogen bond acceptor group in a position equivalent to that observed in the solid state studies of this group of 19 strongly active compounds [4,22].

The present study indicates that the $Ca^{2+}$ channel activators form multiple N(1)-H contacts. Bay K 8644, CGP 28 392 and Bay K 8643 have three contacts each, while Bay O 8495, Bay O 9507 and PN 202791 have two contacts less than 3.5 Å. These interactions are, in contrast to observations made with the antagonists, widely distributed ± 60 degrees along an arc centered on the N(1)-H bond in the N(1)-C(4) vertical plane of the 1,4-DHP ring (Fig. 3). We speculate that the open channel state, to which the activators preferentially bind, either has multiple hydrogen bonding acceptor groups for this N(1)-H donor or that there may be a mobile acceptor site perhaps associated with the dynamics of the channel permeation process. These observations may be incorporated into our previously expressed model of 1,4-DHP interaction at the $Ca^{2+}$ channel [22].

### *Characteristics of the voltage-gated channel*

The sequence-derived model of the voltage-gated $Ca^{2+}$ channel consists of four domains each containing six or more transmembrane α-helices presumably organized around a central pore [23,26]. The fourth α-helix in each of the four domains, labeled the S4 segment, is unusual since it

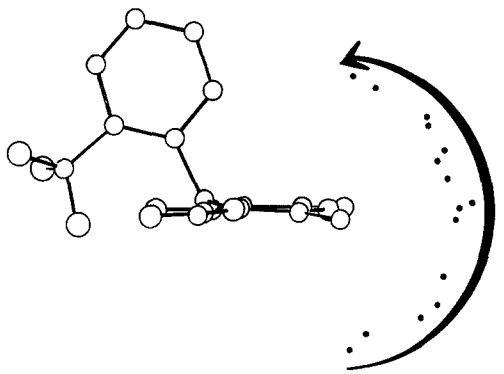

Fig. 3. Lateral view illustrating the variation seen in the positions of the DHP amine acceptor groups determined from the solid state structures of six nifedipine activator analogues. Three structures have three contacts each, the other three have two such contacts less than 3.5 Å. These points are distributed along the arc shown in the N(1)-C(4) vertical plane.

consists of a regularly repeating pattern of five or six positively charged lysine or arginine residues, each separated by two nonpolar residues. The arginine and lysine residues are presumably hydrogen bonded to an encircling group of parallel and antiparallel adjacent α-helices which form a transmembrane portion of the $Ca^{2+}$ channel. Homologous α-helical arrangements are found in other voltage-gated channels, and this unique structure may represent the voltage-sensor. Accordingly, the sliding helix model proposes that the S4 segments are inwardly or outwardly displaced in a helical motion to similar hydrogen-bonded environments in response to polarizing or depolarizing signals, respectively, with the corresponding transfer of gating charges [26]. Because 1,4-DHP interactions with $Ca^{2+}$ channel function are strongly voltage-dependent, we have proposed a model whereby binding to the S4 segment is determinant to activity [22].

*The 1,4-DHP binding site model*

In brief, this model (Figs. 4a and b) assumes that the packing arrangements of helices which span the cell membrane are a square net motif based on the four α-helix bundle, rather than a hexagonal close-packed network. The H-bonding contacts between the S4 helix and the surrounding α-helices cannot be exclusively direct salt bridges because of the 6-fold projection symmetry of the arginine and lysine side-chain positions on the S4 helix and the 4-fold symmetry of the helical packing arrangement (Fig. 4b). The critical features of this model are that binding sites for 1,4-DHP analogues exist in grooves in the S4 helix that are defined by Arg-X-X-Arg sequences on the S4 strand (where Xs are hydrophobic nonpolar residues). The aryl ring of the 1,4-DHP inserts into the helical groove between the two arginine residues with its *para*-position against the helical backbone (Fig. 4c). Hydrogen bonds form between the keto oxygen atoms of the two synperiplanar-oriented ester groups at C(3) and C(5) of the 1,4-DHP ring and the terminal N(η) nitrogen atoms of the guanidyl side chains of the arginine residues. The π-resonant planes of the guanidyl ions stack parallel on either side of the aryl ring to further define this helical cleft. Although a number of separate Arg-X-X-Arg binding clefts may exist on any particular S4 strand, it may be noted that only a few of these will possess a local staggered H-bonded environment which will be conducive to ligand binding (Figs. 4b and c). In the staggered conformation an Arg-X-X-Arg heli-

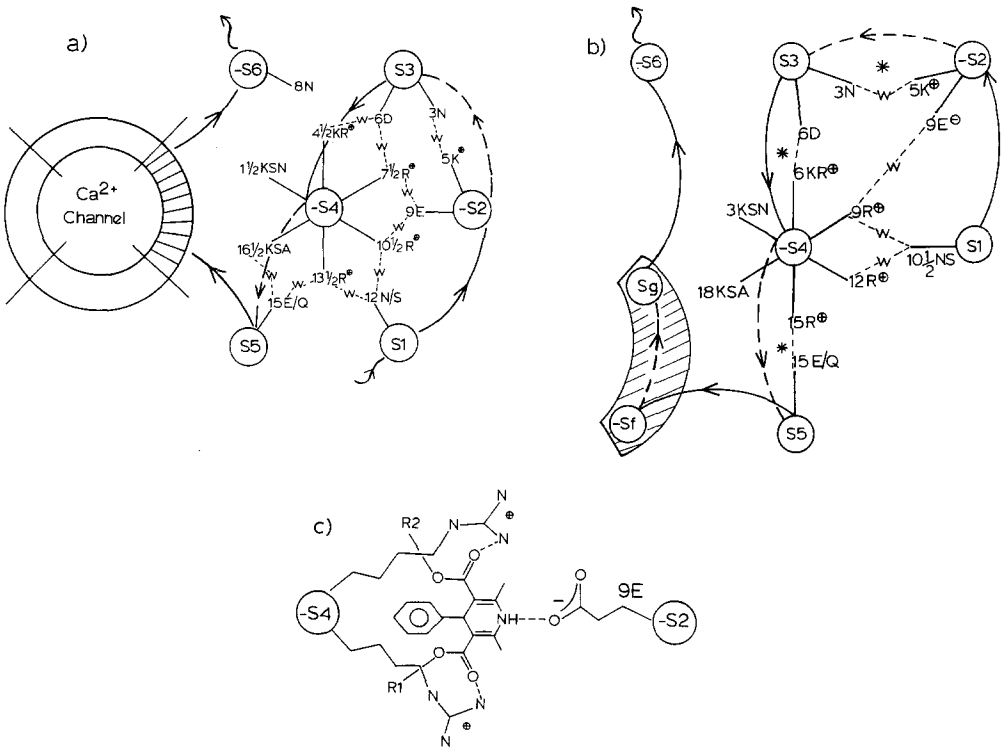


Fig. 4. Diagram of an extracellular view of a hexagonal-packed hydrogen-bonded arrangement of α-helices around an S4 sensor (a) as compared to a square-packed pattern involving a combination of direct salt bridges (*) and water-mediated hydrogen bonds (–W–) (b). Helix labels S1 through S6 are the original assignments of Numa [23], Sf and Sg are short α-helices or β-sheets that have subsequently been described [27,28]. Even numbered helices are preceded with a (–) sign to indicate that the N-to-C-terminal direction reverses in passing from the extracellular to cytoplasmic side of the lipid bilayer. Essential hydrogen bonding groups are indicated by the one-letter symbol of the amino acid residue and a number (1–20) which gives the radial position and relative residue height from the cytoplasmic face of the bilayer. (c) Depicts a nifedipine analogue bound to the 1,4-DHP binding site.

cal cleft will be predisposed to bind to a nifedipine analogue and orient its N(1)-H bond directly at an acceptor group in an adjacent helix. We assume that this hydrogen bond is critical to stabilizing the S4 helix in an antagonist-sensitive nonpermeating gating state. Additionally, the alkyl groups of the C(3) and C(5) ester substituents of these ligands interact by inserting into two distinct binding pockets formed in the surface of the S4 helix by the methylene arms of each arginine residue and a port (P) or starboard (S) amino acid side chain located four residues away in the C-terminal direction (i.e., -Arg-X-X-Arg-P-X-X-S-). Differences in these port and starboard pockets may attribute to the quantitative and qualitative differences in 1,4-DHP activity including their activator/antagonist expression and their tissue selectivity.

*Importance of the molecular electrostatic potential*

The importance of the binding regions in the C(3) and C(5) regions was noted by Höltje and Marrer [29], who reported that differences in the molecular electrostatic potentials between acti-

vator and antagonist structures may constitute the mechanism by which the receptor distinguishes between activator and antagonist ligands. $Ca^{2+}$ channel activators were reported to exert a strong negative potential in the region adjacent to their C(3) nitro substituent while antagonists exhibited a positive potential in this region when an ester group replaced this nitro substituent. In a previous study [30] tryptophan, lysine and phenylalanine were identified as the most probable and important residues for antagonist binding on the basis of force-field and quantum chemical calculations. This 3-site binding model positioned the indole side chain of tryptophan in the region of the electrostatic potential sensor. The potential in the region of this indole was decreased by the proximity of the C(3) nitro substituent of an activator, and increased by the presence of the ester group of an antagonist. According to this model the forces exerted on the indole side chain were presumed to affect the structure of the $Ca^{2+}$ channel protein and alter the permeability of the channel, but were not specific as to how this may have been achieved.

We note that although the reported skeletal muscle $Ca^{2+}$ channel sequence [23] has 10 distinct Arg-X-X-Arg-P-X-X-S regions in its four S4 helices, none of these has an aromatic amino acid at positions P or S which could favorably interact according to this electrostatic potential model. It remains to be re-examined whether other nonaromatic residues appearing at the P and S positions of the published S4 sequences are capable of generating an appropriate interactive potential at these sites. We now consider that such interactions might translate into two separate states, stabilized by activators and antagonists, respectively. Thus in a sequence $Arg_1$-X-X-$Arg_2$-P-X-$Arg_3$-Z-X-X-S, residue Z defines an ester-binding pocket which is shared by two adjacent binding clefts, namely $Arg_1$-X-X-$Arg_2$-P-X-X-Z where Z defines the starboard ester-binding pocket, or conversely, $Arg_2$-X-X-$Arg_3$-Z-X-X-S where Z now indicates the portside pocket position. If residue Z were comparable to tryptophan with regard to exerting a favorable electrostatic potential, the (*R*)- and (*S*)-enantiomers of Bay K 8644 could bind in an exclusive manner to either the $Arg_1$-$Arg_2$ or $Arg_2$-$Arg_3$ clefts, respectively. The chiral selectivity of (*R*)-and (*S*)-Bay K 8644 for these respective binding clefts is illustrated in Fig. 5, where, for the point of emphasis, the Z residue is modeled as a tryptophan shared by two adjacent potential binding clefts.

*Agonist/antagonist gating state interactions*

The activator/antagonist preference of the channel protein will depend upon which of the two adjacent binding clefts is positioned by the S4 rotor in the eclipsed H-bonded cavity (Figs. 4b and c). According to the sliding helix model, where the S4 segment undergoes a 60-degree left-handed outward displacement in response to membrane depolarization [26], one potential binding cleft will be positioned opposite to the N(1)-H acceptor group in the staggered H-bonded receptor cavity during the resting, closed state and a second binding cleft slid into the position of the binding cavity during the depolarized, open state of the channel. Thus the $Arg_1$-X-X-$Arg_2$ binding cleft could be positioned opposite to the binding cavity during the closed state, and upon depolarization the S4 segment would shift outward to its next H-bonded location to now position the $Arg_2$-X-X-$Arg_3$ cleft in the previous binding cavity. Note that the C- to N-terminal direction of the S4 α-helices is known to point outward from the cytoplasmic side to the extracellular side of the membrane [23]. Thus the positioning of these adjacent binding clefts with regard to the open and closed states of the channel is consistent with the observed chirality of activator/antagonist interactions for Bay K 8644 and PN 202 791 which possess the C(3) nitro group. Since this nitro group will form stronger hydrogen bonds than its ester companion, an asymmetry in the bonding of the

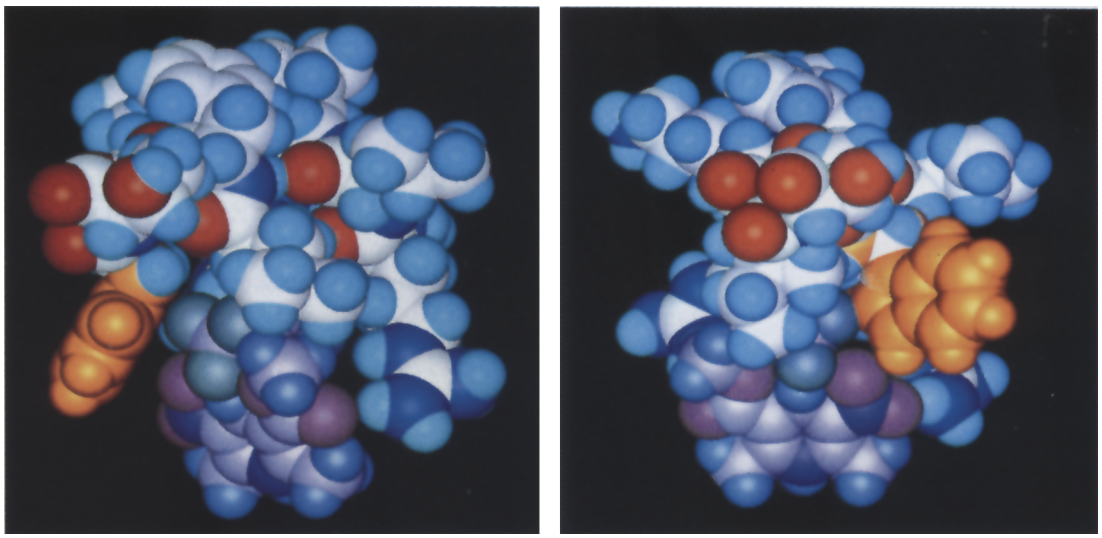

Fig. 5. Space-filling illustrations of the (*R*)- and (*S*)-enantiomers of Bay K 8644 binding to adjacent reading frames $Arg_1$-X-X-$Arg_2$-X-X-$Arg_3$-Trp which share the same Trp residue. The antagonist (*R*)-enantiomer (left) binds to the $Arg_1$-X-X-$Arg_2$-P-X-X-Trp cleft and has the Trp side chain (orange) located in the starboard side ester-binding pocket next to the 3-nitro DHP substituent of the drug. The activator (*S*)-enantiomer (right) may prefer to bind to the adjacent $Arg_2$-X-X-$Arg_3$-Trp-X-X-S binding cleft that would position its 3-nitro DHP substituent next to the same Trp side chain, but which would now appear in the portside ester-binding pocket of this reading frame. The relative positions of these two binding clefts is consistent with the molecular level gating state model described in the text. The antagonist binding cleft, which would be positioned in the receptor cavity during the polarized resting state of the channel, would be shifted one reading frame in the extracellular direction as a consequence of membrane depolarization, and the adjacent agonist binding cleft would be shifted into the receptor cavity as a consequence.

C(3) and C(5) substituent groups of the ligand may occur. This may result in the aryl ring being positioned within the hydrophobic cleft with sufficient flexibility to tolerate the presence of a *para*-substituent on the phenyl ring (compound Bay O 9507).

## CONCLUSIONS

Nifedipine $Ca^{2+}$ channel activators and antagonists share many common structural and conformational features that allow them to bind to the same 1,4-DHP receptor, albeit to different gating-state receptor conformations. The potency of Bay K 8644 analogue activators is not as critically dependent on DHP ring planarity or the absence of a bulky *para*-group on the 4-phenyl DHP ring substituent as was previously noted for the potency of nifedipine antagonists of the L-type voltage-dependent $Ca^{2+}$ channel. Diffraction analyses reveal that the hydrogen-bond acceptors to the DHP amine of Bayer activators are not restricted to a single significant interaction which is polarized along the line of sight of the N(1)-H bond as was noted for antagonists. Bayer activators tend to have multiple DHP-amine contacts which are uniformly distributed $\pm$ 60 degrees from the N(1)-H bond in the vertical N(1)-C(4) plane of the DHP ring. This flexibility of

bonding to the amine acceptor group may have consequences with regard to activator ligands binding to the ion conducting open channel state. The molecular electrostatic potential may be an important factor which induces activator and antagonist ligands to bind to different, albeit adjacent binding clefts on the S4 α-helix. The selection of (*S*)- and (*R*)- Bay K 8644 enantiomers for the respective open and closed-inactivated states of the channel is consistent with the relative positions of adjacent binding clefts sharing a common electrostatic potential sensor and their inferred gating state positions with respect to the receptor cavity. Whether or not nonaromatic amino acids can induce a favorable electrostatic potential for this purpose remains to be examined. Affinity labeling and point site mutagenic studies will provide experimental evidence for molecular level hypotheses that detail how the 1,4-DHP receptor is affected by voltage-gating and how the $Ca^{2+}$ channel is predisposed for binding activator and antagonist ligands in the appropriate gating state conformations.

## ACKNOWLEDGEMENTS

We thank Dr. Horst Meyer of Bayer A.G., Wuppertal, for kindly providing samples of the activator analogues used in this study. Assistance by Dr. G.D. Smith with the computer graphics is much appreciated. Support of this project from the National Institutes of Health (HL16003 and HL32303) is gratefully acknowledged.

## REFERENCES

1 Schram, M., Thomas, G., Towart, R. and Franckowiak, G., *Nature (Lond.)*, 303 (1983) 535.
2 Janis, R.A., Rampe, D., Sarmiento, J.G. and Triggle, D.J., *Biochem. Biophys. Res. Commun.*, 121 (1984) 317.
3 Janis, R.A., Silver, P. and Triggle, D.J., *Adv. Drug Res.*, 16 (1987) 309.
4 Triggle, D.J., Langs, D.A. and Janis, R.A., *Med. Res. Rev.*, 9 (1989) 123.
5 Loev, B., Goodman, M.M., Snader, K.M., Tedeschi, R. and Macko, E., *J. Med. Chem.*, 17 (1974) 956.
6 Rodenkirchen, R., Bayer, R., Steiner, R., Bossert, E., Meyer, H. and Möller, E., *Naunyn-Schmied. Arch. Pharmacol.*, 310 (1979) 69.
7 Rodenkirchen, R., Bayer, R. and Mannhold, R., *Prog. Pharmacol.*, 5 (1982) 9.
8 Triggle, A.M., Shefter, E. and Triggle, D.J., *J. Med. Chem.*, 23 (1980) 1442.
9 Fossheim, R., Svarteng, K., Mostad, A., Rømming, C., Shefter, E. and Triggle, D.J., *J. Med. Chem.*, 25 (1982) 126.
10 Coburn, R.A., Wierzba, M., Suto, M.J., Solo, A.J., Triggle, A.M. and Triggle, D.J., *J. Med. Chem.*, 31 (1988) 2103.
11 Rampe, D. and Triggle, D.J., *Trends Pharmacol. Sci.*, 7 (1987) 461.
12 Franckowiak, G., Bechem, M., Schram, M. and Thomas, G., *Eur. J. Pharmacol.*, 114 (1985) 223.
13 Wei, X.Y., Luchowski, E.M., Rutledge, A., Su, C.M. and Triggle, D.J., *J. Pharmacol. Exp. Therap.*, 239 (1986) 144.
14 Hof, P.R., Rüegg, U.T., Hof, A. and Vogel, A., *J. Cardiovasc. Pharmacol.*, 7 (1985) 689.
15 Gjörstrup, P., Hårding, H., Isaksson, R. and Westerlund, C., *Eur. J. Pharmacol.*, 122 (1986) 357.
16 Fossheim, R., Joslyn, A., Solo, A.J., Luchowski, E., Rutledge, A. and Triggle, D.J., *J. Med. Chem.*, 31 (1988) 300.
17 Langs, D.A. and Triggle, D.J., *Mol. Pharmacol.*, 27 (1985) 544.
18 Fossheim, R., *Acta Chem. Scand.*, B41 (1987) 581.
19 Kwon, Y.W., Franckowiak, G., Langs, D.A., Hawthorn, M., Joslyn, A. and Triggle, D.J., *Naunyn-Schmied. Arch. Pharmacol.*, 339 (1989) 19.
20 Enraf-Nonius, *Structure Determination Package*, Enraf-Nonius, Delft, 1979.
21 Stout, G.H. and Jensen, L.H., *X-ray Structure Determination*, Macmillan, New York, 1968, p. 457.
22 Langs, D.A., Strong, P.D. and Triggle, D.J., *J. Comput.-Aided Mol. Design*, 4 (1990) 215.
23 Tanabe, T., Takeshima, H., Mikami, A., Flockerzi, V., Takahashi, H., Kangawa, K., Kojima, M., Matsuo, H., Hirose, T. and Numa, S., *Nature (Lond.)*, 328 (1987) 313.

24 Mahmoudian, M. and Richards, W.G., *J. Chem. Soc. Commun.*, (1986) 739.
25 Rovnyak, G., Andersen, N., Gougoutas, J., Hedberg, A., Kimball, S.D., Malley, M., Moreland, S., Porubcan, M. and Pubzianowski, A., *J. Med. Chem.*, 31 (1988) 936.
26 Catterall, W.A., *Science*, 242 (1988) 50.
27 Guy, H. R. and Seetharamulu, P., *Proc. Natl. Acad. Sci. USA*, 83 (1986) 508.
28 Greenblatt, R.E., Blatt, Y. and Montal, M., *FEBS Lett.*, 193 (1985) 125.
29 Höltje, H.-D. and Marrer, S., *J. Comput.-Aided Mol. Design*, 1 (1987) 23.
30 Höltje, H.-D. and Marrer, S., *Quant. Struct.-Act. Relat.*, 7 (1988) 174.